# Evidence accumulation during perceptual decision-making is sensitive to the dynamics of attentional selection

*Running title:* Decision making depends on attentional selection

*Authors:* Dragan Rangelov[a] and Jason B. Mattingley[a,b]

*Affiliations:*

[a]Queensland Brain Institute, The University of Queensland, St Lucia, QLD 4072, Australia

[b]School of Psychology, The University of Queensland, St Lucia, QLD 4072, Australia

*Corresponding Author:* Dragan Rangelov, d.rangelov@uq.edu.au, +61 401 281 181

*Conflict of interest:* The authors declare no competing financial interests.

*Abstract*

The ability to select and combine multiple sensory inputs in support of accurate decisions is a hallmark of adaptive behaviour. To date, most studies of perceptual decision-making have involved tasks in which observers made judgements on task-relevant stimuli only. In the real world, however, mechanisms of attention are often needed to prioritize stimuli that are task-relevant and to attenuate potentially distracting sources of sensory information. According to sequential-sampling decision-making models, selective attention should modulate evidence accumulation by filtering out task-irrelevant inputs. To test this notion, we developed a novel 'integrated' decision-making task, in which participants judged the average direction of successive target motion signals while ignoring concurrent and spatially overlapping distractor motion signals. We recorded neural activity using electroencephalography, and used computational modelling approaches to determine whether evidence accumulation is influenced by attentional selection. We found that while target stimuli strongly influenced perceptual decisions and associated neural activity, concurrent and spatially coincident distractor stimuli also exerted a measurable bias on integrated decisions and neural evidence accumulation. Our findings suggest that attentional selectivity dynamically modulates decision weights derived from evidence accumulation processes, and that attention operates as a real-time but imperfect filter between perception and decision making.

*Author summary*

The ability to decide on the basis of multiple goal-relevant signals while ignoring distractors is a hallmark of adaptive, intelligent behaviour. While attention and decision-making processes have been well characterised in isolation, relatively little is known about how the two interact. Here we developed a novel paradigm in which participants had to integrate task-relevant sensory inputs over periods of noise while disregarding distractor signals. We demonstrate a profound influence of selective attention on behavioural and electrophysiological measures of decision-making, and show that feature-based attention operates as an imperfect, real-time filter between sensory inputs and decision-making processes.

## *Introduction*

Cognition can be conceived of as a cascade of processes, beginning with the encoding of sensory input and ending with appropriate behavioural choices. Sequential-sampling decision-making models have had considerable success in describing choice behaviour in terms of both behavioural performance and neural activity (1–3). According to these models, decision-making relies on a central decision variable, an abstract quantity that accumulates in time toward one of several possible choice alternatives. On these accounts, a choice is made once the decision variable reaches threshold. In one widely employed decision-making task – the random-dot motion discrimination task (2,4) (see Fig. 1a) – participants are shown fields of randomly moving dots and are asked to judge the motion direction of a fraction of the dots that move coherently. Studies in both animals (4) and humans (5–10) have shown that neural activity recorded during random-dot motion discrimination follows a trajectory that resembles the accumulation of a decision variable, thereby lending neurobiological support to sequential-sampling decision-making models.

To date, much has been learned about simple perceptual decision-making in humans and other animal species (3,11,12). In the real world, however, decisions are often more complex, requiring judgements on stimuli that are separated in time and space, and which may or may not be task relevant. For example, deciding to cross a busy road requires us to integrate the motion directions of vehicles coming from both the left and right sides, while disregarding any movements made by people or objects on the sidewalk. Relatively little is known about how the brain regulates decision-making when it receives competing – task-relevant and irrelevant – sensory inputs. According to sequential-sampling decision-making

models, selective attention should mediate sensory input and evidence accumulation, presumably filtering out task-irrelevant inputs and preventing them from being accumulated into the decision variable (13–16). This framework raises at least two inter-related questions. First, what is the relationship between the time-course of attentional selection and evidence accumulation, and second, how effective is attention in mediating sensory encoding and evidence accumulation? Conceptually, selection and accumulation could take place sequentially so that only prioritised, task-relevant input is accumulated. Alternatively, the two processes could take place in parallel, so that task-irrelevant inputs might also impact upon evidence accumulation to some extent, particularly in the early stages of attentional selection.

In recent years there has been increased interest in studying behaviour and neural activity in more complex decision-making tasks (14,16–22). To increase decision complexity, many of these studies have varied the number of response alternatives (e.g., two vs. four), and have found significant costs associated with a larger number of potential responses (e.g., Churchland et al., 2008; Leite and Ratcliff, 2010; Itthipuripat et al., 2018; Kohl et al., 2018). As increasing response alternatives also normally requires an increase in the number of target stimuli, it remains unclear which processing stages – from early target selection to later response execution – are impacted by such increases in decision complexity.

Here we took a different approach by seeking to measure the effects of attention on the dynamics of evidence accumulation using a novel task in which observers monitored concurrent task-relevant and task-irrelevant visual stimuli. Across two experiments, we used random-dot displays (Fig. 1a) comprising *two* simultaneous, intermingled fields of dots, one

in a cued (target) colour, the other in an uncued (distractor) colour. We presented two epochs of concurrent target/distractor motion, and participants were asked to reproduce the *average motion direction* of successive target-coloured dots, ignoring the directions of any concurrent distractor dots. Thus, unlike the classical random-dot motion task in which participants judge the direction of a single coherent motion target presented in isolation, here they had to integrate sensory evidence from successive target motion stimuli to determine their average direction, while trying to ignore the directions of concurrent distractor dots. The averaging task enabled us to characterise the degree to which task-relevant and task-irrelevant signals contribute to perceptual decision-making, and to investigate the temporal integration of these discrete motion signals into a single, integrated perceptual decision.

*Results*

In Experiment 1, a group of 36 participants judged the average motion direction of target-coloured dots across three successive epochs within each trial (Fig. 1a). To quantify task performance, we computed error magnitudes (Fig. 1b) by subtracting the true average motion direction from the reproduced direction. The distributions of error magnitudes per experimental condition were used to estimate the response precision ($K$) and guessing rates ($\alpha$), which reflect how well participants performed the task and how often they guessed, respectively. As initial analyses showed no differences between repetitions and changes of target colour within a trial (all ts < 1), these two trial types were averaged for further analyses.

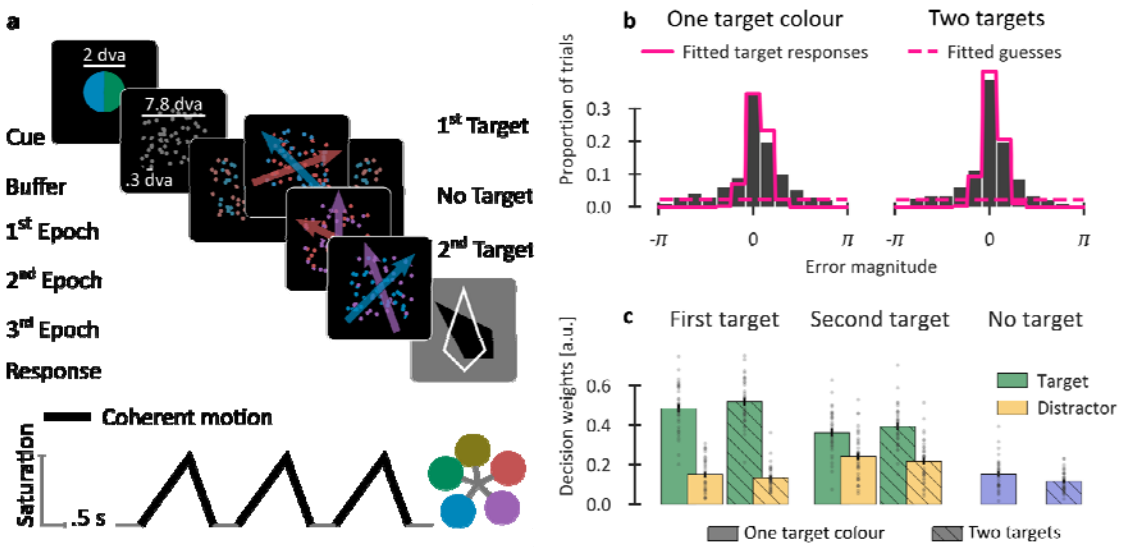


**Figure 1. Schematic of the stimuli, task and the behavioural results in Experiment 1. a,** Example stimulus sequence from a typical trial (above) together with the timing of colour saturation modulation and coherent-motion onsets (below). Participants had to reproduce the *average* motion direction of target-coloured dots by adjusting the orientation of a response dial (black pointer). After indicating their response they received feedback on accuracy within the same display (white pointer). **b,** Group-level histograms (bars) of the error magnitude (reproduced motion direction minus expected). The pink lines show fitted distributions of target responses and guesses using mixture-distribution modelling of each individual participant's data. **c,** Average decision weights showing the contributions of each presented motion direction to the decision. Since there were no significant differences ($t < 1$) between the two non-target motions in the "No target" condition (blue bars), only the average of the two is shown. Grey dots denote individual participants.

The average response precision was high both in the one- and two-target colour conditions ($K_{M/SEM}$ = 10.52/1.70 and 11.79/2.08), and did not differ significantly between conditions ($F < 1$). Overall, the full-width-at-half-maximum (FWHM) of the fitted distribution of target responses was around 40°. For reference, the average tuning width of individual neurons in macaque area MT is about 60° FWHM (31). The average guessing rates ($\alpha$) were around 26%, and did not change across experimental conditions ($F < 1$).

121 To quantify how much each of the presented target and distractor signals influenced
122 observers' average-motion decisions, we used linear regression modelling with complex-
123 valued data (see Methods). The decision weights for all motion signals in all experimental
124 conditions were significantly different from zero (all $p < .001$), indicating that both task-
125 relevant and task-irrelevant signals contributed to the decision. As with the mixture
126 distribution modelling, initial analyses of decision weights revealed no significant
127 differences between target colour repetitions and changes (all Fs < 1.97, all ps > .170), so
128 the two conditions were averaged for further analyses. Overall, the weights for targets
129 (.44/.01, Fig. 1c) were much higher ($F_{2,64} = 326.80$, $p < .001$, $\eta_p^2 = .91$) than the weights for
130 either concurrently presented distractors (.19/.01) or distractors presented on their own
131 (.13/.01). Unexpectedly, there was also a reliable order effect, with higher target weights for
132 the first epoch than for the second (.50/.01 vs. .38/.02, $t_{32} = 4.74$, $p < .001$); analogously,
133 distractor weights were lower for the first epoch than for the second (.14/.01 vs. .23/.01, $t_{32}$
134 $= 4.68$, $p < .001$). Overall, the analyses of decision weights revealed that attention operates
135 as an imperfect filter between sensory input and evidence accumulation by attenuating,
136 rather than eliminating, the weights associated with task-irrelevant inputs.

137 We next characterised the temporal dynamics of evidence accumulation. To this
138 end, we inspected the CPP ERP component whose time-course has been shown to closely
139 follow evidence accumulation (3,8–10,32). We were particularly interested in the CPP in no-
140 target epochs: if attentional selection and evidence accumulation operate sequentially, then
141 attention should suppress motion signals, predicting no CPP in this epoch. By contrast, if

selection and accumulation take place concurrently, there should be a significant CPP even in the no-target epoch.

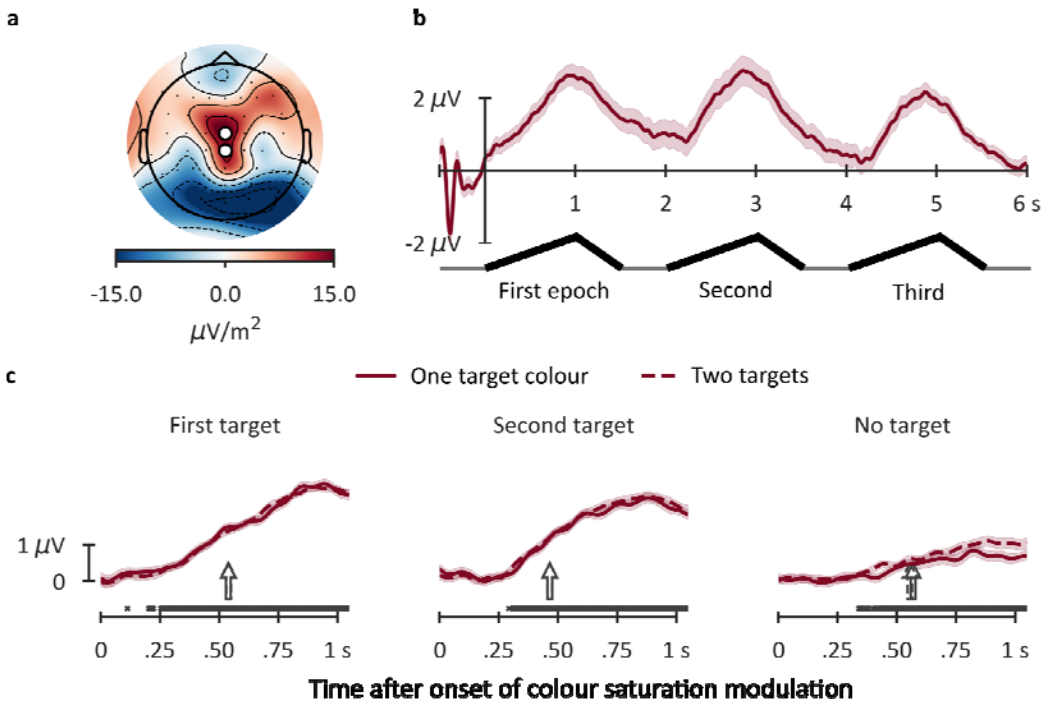


**Figure 2. Topography and time course of the CPP component in Experiment 1. a,** Surface-Laplacian-filtered EEG topography averaged across all conditions at times of peak colour saturation for all three epochs (1, 3, and 5 s after stimulus onset). The markers denote the electrode pair [CPz and Cz] used for the ERP analyses. **b,** Time-course of the CPP averaged across all experimental conditions (M ± 1 within-participants SEM; Morey, 2008) for the total trial duration. **c,** CPP time-course during the gradual increase in colour saturation, shown separately per epoch and experimental condition. Symbols above the x-axis denote time samples for which the voltage was significantly different from 0 at $p_{FDR} < .05$. Full-line and dashed-line arrows indicate onset latencies in the one and two target colours conditions, respectively. For the purpose of data presentation, all traces were low-pass filtered at 10 Hz using a $4^{th}$ order Butterworth IIR filter. Data analyses were conducted using unfiltered data.

Inspection of the ERP topographies (Fig. 2a) revealed a central-medial positivity consistent with the usual CPP component (8). Throughout the trial, the CPP (Fig. 2b) closely

157 followed the time-course of colour modulation, with three distinct peaks coinciding with the
158 three episodes of maximum colour saturation. Between epochs, as the colour saturation of
159 the dots returned to grey, the CPP amplitude also returned close to baseline. This pattern
160 suggests that evidence was accumulated only during the informative time periods, and
161 implies a strong effect of attention on evidence accumulation. If evidence had accumulated
162 throughout the trial irrespective of task-relevance, we would have expected a sustained CPP
163 response, which clearly was not the case.

164 Next, the whole-trial epochs were divided into three segments relative to the onset
165 of colour saturation modulation, and baseline-corrected relative to the average of all three
166 epochs over a window of 100 ms prior to onset. Thus, all three epochs had the same
167 baseline, permitting comparisons between them. The epochs were then sorted according to
168 experimental conditions (first target, second target, no target; one- and two-target colours)
169 and averaged across trials. As with the behavioural findings, we observed no effects of
170 target colour repetitions vs. changes (all $F_c < 1$). Further analyses were therefore conducted
171 using the average of the two trial types. Overall, there was a statistically significant positive
172 deflection in all experimental conditions (Fig. 2c). The onset latency (522 ms) and the CPP
173 slope (3.31 μV/s) were similar across experimental conditions (all $F_c < 1$), suggesting that the
174 rate of evidence accumulation did not differ between conditions. The peak CPP amplitude,
175 however, *decreased* between epochs ($F_{c(2, 64)} = 46.41$, $p < .001$), from the first target epoch
176 to the second and then to the no-target epoch (2.74, 2.43 and 1.06 μV, respectively, all $t_{c(32)}$
177 $\geq 1.93$, $p \leq .031$). Finally, the number of target colours had no significant effect on the peak

178 CPP amplitude, either as a main effect ($F_c < 1$) or in combination with epoch ($F_{c(2,64)} = 1.44$, p
179 = .244).

180 Taken together, the results of Experiment 1 revealed strong effects of selective
181 attention on decision-making. At the neural level, attention had a robust effect on the peak
182 CPP amplitude, with higher peaks for target-present epochs than for no-target epochs.
183 Behaviourally, target signals were associated with significantly larger decision weights than
184 distractors. Importantly, however, neither the CPP onset nor the slope differed between
185 target-present and no-target epochs, suggesting that both task-relevant and task-irrelevant
186 inputs triggered evidence accumulation processes. Moreover, there was a robust and
187 significant influence of distractor events on behaviour, suggesting that attention does not
188 fully attenuate irrelevant inputs. Overall, the results are consistent with a view that
189 attentional selection and evidence accumulation take place concurrently, with attention
190 mediating sensory processing and decision-making.

191 In Experiment 1, we used an increase in colour saturation to gradually reveal to
192 participants the task-relevance of the overlapping motion stimuli, and to render the
193 coherent motion signals discernible. While this design was clearly effective for measuring
194 the impact of distractors on decision making, is possible that attentional filtering of
195 distractors might have been more successful if participants had been given an opportunity
196 to fully select the task-relevant stimuli (cued target colour) prior to the onset of coherent
197 motion events. To test this hypothesis, in Experiment 2 the trial epochs were structured so
198 that the colours of the dot stimuli reached full saturation prior to the onset of coherent
199 motion events, thus effectively separating selection-related and decision-related signals in

time. Specifically, in Experiment 2 a new group of 36 participants viewed displays in which the saturation of the target and distractor dots was initially ramped to maximum within each epoch of the trial. The coherent motion events were then presented for .5 s at a jittered interval during the period of maximum saturation (see Fig. 3a).

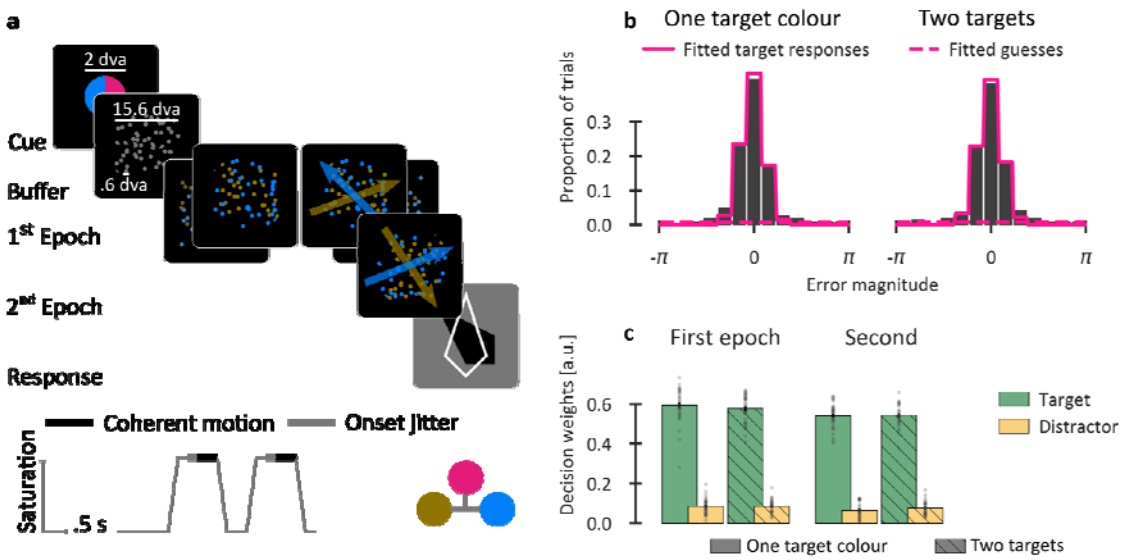


**Figure 3. Schematic of the stimuli, task and the behavioural results in Experiment 2. a,** Example stimulus sequence from a typical trial (above) together with the timing of colour saturation modulation and coherent-motion onsets (below). Only target-present epochs were presented, and the increase in colour saturation and onset of coherent motion were separated in time. Dot patches were frequency-tagged at 12 and 18 Hz (counterbalanced across target and distractor stimuli). **b,** Group-level histograms (bars) of the error magnitude together with the best-fitting mixture-distribution models (pink lines). **c,** Average decision weights showing the contributions of each presented motion direction to the decision. Grey dots denote individual participants.

To independently monitor the brain's responses to target and distractor motion, the two sets of dots were flickered at different frequencies (12 and 18 Hz). Using a similar approach, studies on visual attention have shown (34,35) that when two differently-coloured, spatially overlapping random-dot patches are presented, electrophysiological

responses to the task-relevant, target patch are stronger than those to concurrent distractor stimuli. Unlike previous studies, the design of Experiment 2 enabled us to track attentional deployment within a trial as a function of stimulus discriminability. Specifically, we were able to independently characterise the brain's responses to target and distractor patches prior to, during, and after the modulation of colour saturation. Since the flickering stimuli permitted independent tracking of target and distractor signals, we removed no-target epochs and presented only target-present epochs.

The behavioural results of Experiment 2 were strikingly similar to those of Experiment 1. Initial analyses revealed no effect of repeating vs. changing the target colour (all ts < 1), so all subsequent analyses used the average of the two. Response precision (Fig. 3b) was high and comparable between one- and two-target colour trials ($\mathrm{K}$/FWHM = 7.96/48° and 7.37/50°, respectively, $F_{1,30} = 2.37$, $p = .134$). Likewise, guessing rates were low and virtually identical for one- and two-target colour trials (ca. 12%, $F < 1$). Analyses of decision weights revealed that both target and distractor signals contributed to the average motion-direction response in all conditions (all $p < .001$). The weights (Fig. 3c) for targets, however, were seven times higher than those for distractors (.56/.01 and .08/.01, respectively, $F_{1,30} = 1{,}845$, $p < .001$, $\eta_p^2 = .98$). The serial order effect from Experiment 1 was also replicated, with higher decision weights for the first epoch than for the second, both for targets (.58/.01 vs. .54/.01, $t_{30} = 3.06$, $p = .004$) and distractors (.09/.01 vs. .07/.01, $t_{30} = 3.32$, $p = .002$). Finally, there was no significant difference between one- and two-target colour trials, either as a main effect or in combination with the other factors (all $F \leq 1.35$, all $p \geq .254$).

238 We next characterised the time-course of the CPP. The ERP topography (Fig. 4a) in
239 Experiment 2 was broadly consistent with that of Experiment 1, showing a central-medial
240 positivity. The time-course of the CPP (Fig. 4b) throughout the trial closely followed the
241 modulation of colour saturation, peaking sharply around .8 and 2.8 s and decaying quickly
242 thereafter. There was also a second modulation, broadly coinciding with the coherent
243 motion onsets (at around 1.5 and 3.5 s), which, due to the jittered timing of the motion
244 onsets, rose and fell more slowly than the colour-evoked components. As in Experiment 1,
245 the phasic modulation of the CPP suggests that several episodes of evidence accumulation
246 took place throughout a trial. A single accumulation episode would have yielded a sustained
247 component throughout the trial, which clearly was not the case.

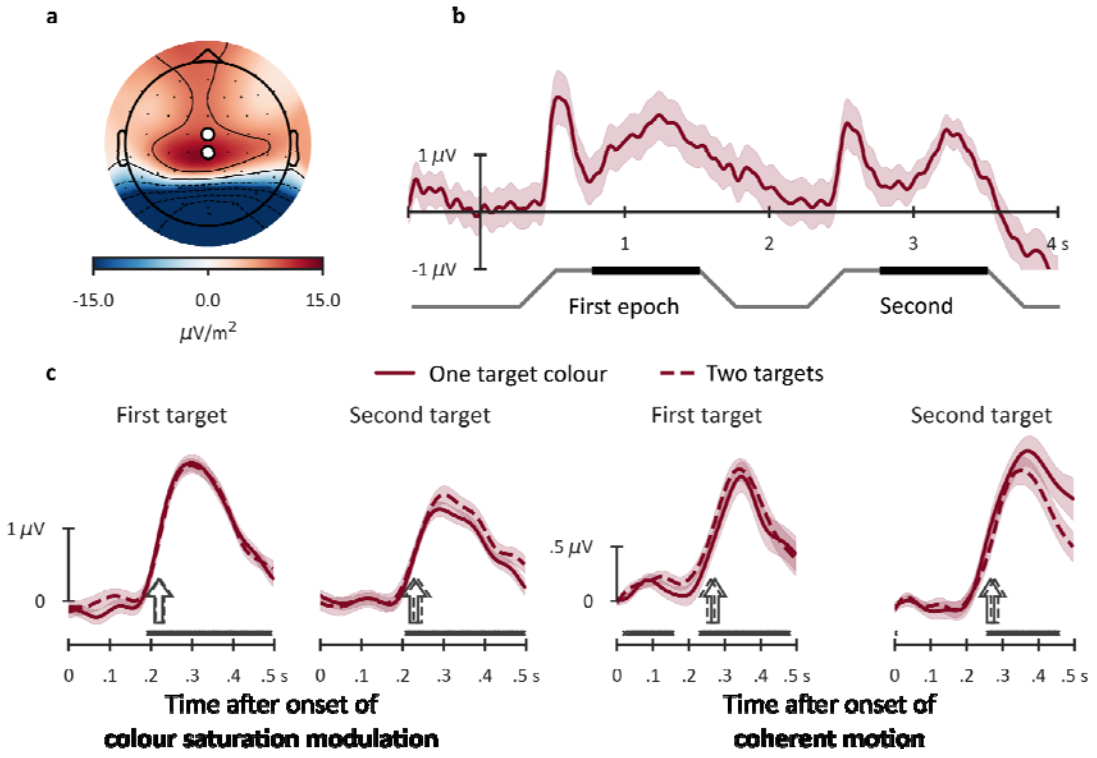


248

249 **Figure 4. Topography and time course of the CPP component in Experiment 2. a,** Surface-Laplacian-filtered
250 EEG topography averaged across all conditions at the middle of peak colour saturation for both epochs. **b,** The

CPP component averaged across all experimental conditions for the total trial duration. **c**, Time-course of the CPP time-locked to the onset of colour saturation (left panels), and to the onset of coherent motion (right panels), shown separately per epoch and experimental condition. Note the difference in scale between panels. Conventions as in Figure 2.

Analyses of the CPP (Fig. 4c) time-locked to the onset of colour modulation and coherent motion, respectively, revealed a significant positive deflection in both cases. Analyses of *colour-locked CPPs* for the first epoch relative to the second revealed a shorter onset latency (220 vs. 231 ms, $F_{c(1,30)} = 5.04$, $p = .032$), a marginally steeper slope (17.57 vs. 13.34 μV/s, $F_{c(1,30)} = 3.23$, $p = .083$) and a higher peak amplitude (1.95 and 1.42 μV, $F_{c(1,30)} = 6.40$, $p = .017$). In the second epoch, dividing attention between two target colours yielded a significantly higher peak amplitude for two- versus one-target colour trials (1.56 and 1.29 μV, respectively; $t_{c(1,30)} = 2.30$, $p = .029$) . Analyses of *motion-locked CPPs*, by contrast, revealed no significant differences in onset latency (270 ms), slope (9.44 μV/s) or peak amplitude (1.27 μV) between experimental conditions (all $F_c <= 1.44$, all ps >= .240). Overall, the ERP analyses of Experiment 2 suggest that both selecting the task-relevant colour patch (i.e., attentional allocation) and deciding on the motion direction (i.e., perceptual discrimination) involve some degree of evidence accumulation. Further, as only the colour-locked CPP differed between the first and second epoch, it appears that the serial order effect observed in both Experiments 1 and 2 was more closely related to processing of colours rather than processing of the motion signal itself.

To independently characterise the brain's response to target and distractor signals, we next analysed the amplitude of SSVEP responses elicited by the frequency-tagged motion stimuli. There was a strong (≈2 dB) frequency-specific response which peaked at the

Oz electrode over the occipital pole (Fig. 5a,b). Time-frequency analyses revealed that the power of both target and distractor signals was significantly different from zero throughout the trial (all $p_{FDR\text{-}corrected} < .05$). Moreover, the power was similar for target and distractor patches prior to the increase in colour saturation in both the first and second epochs (Fig. 5c). This suggests that participants divided attention across both patches during periods in which the two patches were indistinguishable.

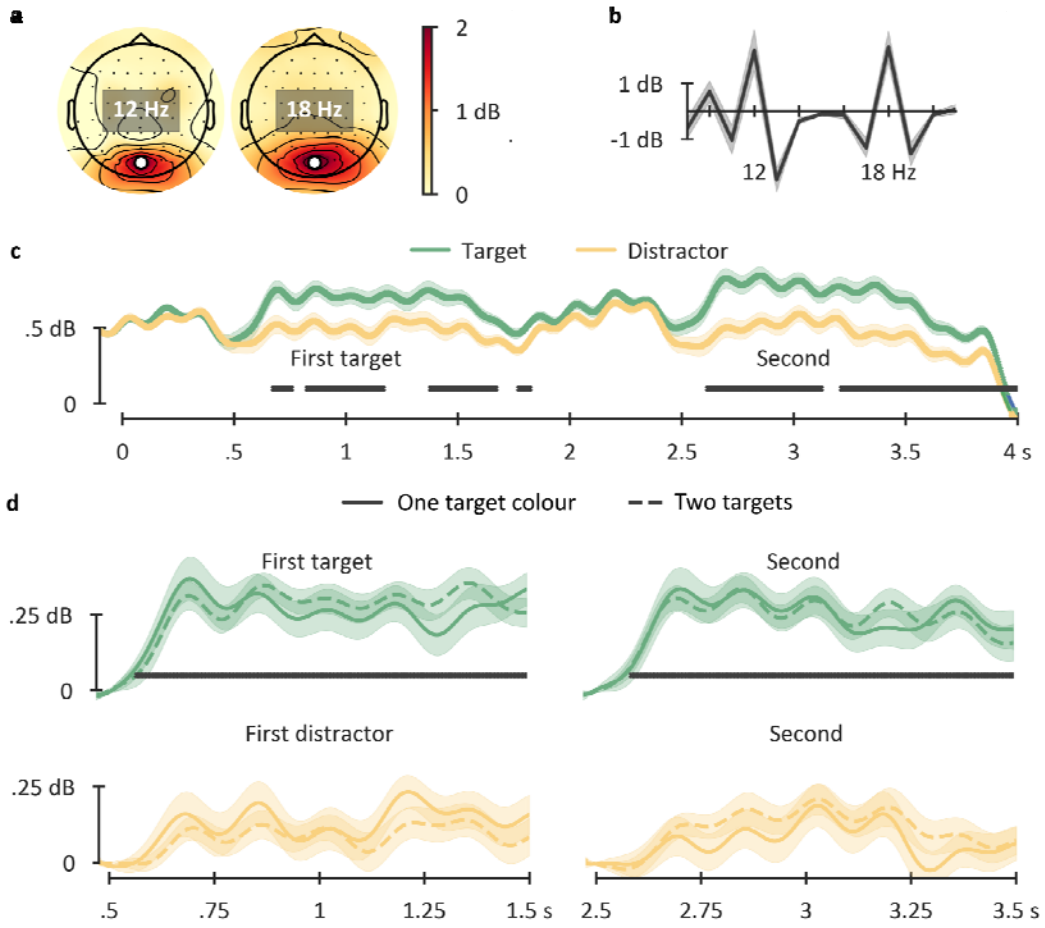


**Figure 5. Time-course of target and distractor processing measured as SSVEP power in Experiment 2. a**, Topography of the total power at 12 Hz and 18 Hz normalized relative to the neighbouring frequencies, computed using a fast-Fourier transform during periods of maximal colour saturation (.5–1.5 s, and 2.5–3.5 s). **b**, Normalized total SSVEP power (M ± 95% CI) at Oz electrode during the period of maximal colour saturation

averaged across epochs and all experimental conditions. **c**, Time-resolved target- and distractor-evoked SSVEPs for the whole trial duration averaged across all experimental conditions (M ± 1 within-participants SEM). Black symbols above the x-axis denote times at which the difference between target and distractor power was significant at $p_{FDR\text{-}corrected} < .05$. **d**, Target-evoked (upper panels) and distractor-evoked (lower panels) SSVEPs per epoch and per experimental condition baseline-corrected relative to .1 s interval around the onset of maximum colour saturation (.5 and 2.5 s for the first and second epoch, respectively). Black symbols above the x-axis denote times at which the baseline-corrected power was significantly different from zero at $p_{FDR} < .05$.

As the colour saturation increased, there was a transient *decrease* in power for the two patches in both the first epoch (around .5 s) and the second (around 2.5 s). Whereas the power for target patches in both epochs recovered quickly (Fig. 5d, upper panels), the power for distractor patches remained unchanged throughout the epochs (Fig. 5d, lower panels), yielding a robust effect of task-relevance (average power: .24 and .10 dB for target and distractor patches, respectively, $F_{1,30} = 11.64$, $p = .002$, $\eta_p^2 = .28$). Finally, the SSVEP power was comparable across the first and second epochs, and across one- and two-target colours (all $F \leq 1.25$, all $p \geq .272$). Taken together, the lower guessing rates and lower decision weights in Experiment 2 relative to Experiment 1 suggest that preparation time improves the selectivity of attentional filters. Nevertheless, both the decision weights and the SSVEPs revealed that distractor signals still evoked brain responses and influenced participants' average motion-direction decisions. In line with Experiment 1, the results of Experiment 2 suggest that selective attention cannot fully prevent task-irrelevant inputs from influencing evidence accumulation.

307 *Discussion*

308 The goal of the present study was to characterise the behavioural and neural
309 processes associated with making integrated perceptual decisions. Unlike simple perceptual
310 decision-making (1,2,36), which requires judgments on a single, task-relevant stimulus, our
311 decision-making task involved selective processing of target signals in the presence of
312 distractors, and required integration of sensory evidence over an extended time period
313 within a trial. To characterise the role of selective attention in decision making, we used
314 mixture distribution modelling and regression analyses. To characterise the neural
315 correlates of decision-making, we used a widely accepted correlate of evidence
316 accumulation in humans, the centro-parietal positivity (CPP) component (3,11,20). Finally,
317 to monitor processing of different, task-relevant and task-irrelevant sensory inputs, in
318 Experiment 2 we flickered stimuli at different frequencies and measured SSVEPs to targets
319 and distractors.

320 The time-course of evidence accumulation, as indexed by CPP amplitude, co-varied
321 with the phasic modulation of colour saturation throughout each trial: the CPP was large at
322 high saturation levels and returned to baseline when the dots desaturated to grey. A single
323 evidence accumulation process would predict a sustained CPP response, whereas our
324 findings suggest that several episodes of evidence accumulation took place within a trial,
325 and these were triggered by the onset of task-relevant stimulus features. Experiment 2
326 revealed a strong CPP evoked by both colour and motion onsets (which were dissociated
327 within each trial), suggesting that the colour and motion signals engaged distinct evidence
328 accumulation processes in support of detecting a task-relevant colour, on the one hand, and

329 discriminating task-relevant motion signals, on the other. These findings are consistent with
330 studies which have used the evidence-accumulation framework to model behaviour in both
331 detection (13) and discrimination tasks (15).

332 The results of the two experiments suggest that selective attention operates as an
333 imperfect, real-time filter between perception and decision-making. Whereas targets had a
334 reliably stronger influence on behaviour and associated neural activity, distractor stimuli
335 also had a measurable influence on decision weights. In Experiment 1 there was a
336 measurable CPP in no-target epochs, suggesting that the onset of any sensory event within
337 a trial, whether target or distractor, triggered an episode of evidence accumulation.
338 Additionally, the robust and significant effect of no-target motion epochs on integrated
339 decisions suggests that participants were unable to suppress these distractor signals from
340 being accumulated. Taken together, the findings of Experiment 1 suggest that perceptual
341 decision making takes place in parallel with attentional selection. At early stages of
342 attentional selection, coherent motion information carried by both the target and distractor
343 patches are accumulated into the decision variable. As attentional selectivity increases, the
344 distractor inputs are attenuated, an observation that is consistent with the lower CPP
345 amplitude and lower decision weights for no-target epochs than target-present epochs.
346 Consistent with Experiment 1, the neural responses to distractors in Experiment 2, while
347 significantly smaller than those to targets, were not completely suppressed and remained
348 stable over the period during which target and distractor patches were discernible within
349 the trial. In Experiment 2, participants had ample time to select the task-relevant patch (> .5
350 s). Despite this, there was a robust distractor effect on responses suggesting that during

351 integrated decision-making tasks attention does not completely suppress the accumulation
352 of task-irrelevant sensory input.

353 Overall, the results of the present study are consistent with the notion that sensory
354 evidence accumulates in parallel (rather than sequentially) with increased selectivity for
355 task-relevant *features*. Computational modelling of response speed and accuracy in the
356 classic flanker task – in which target and distractor stimuli are presented concurrently at
357 different spatial locations (e.g., 37) – has shown that similar principles apply to selectivity
358 for task-relevant *locations* (15). Of note, in a recent study Wyart et al. (2015) had
359 participants report the average orientation of one of two spatially separated streams of
360 achromatic gratings. Unlike the present study, decision weights for the spatially separated
361 distractors were not statistically different from zero. While differences in experimental tasks
362 and analytical approaches prevent direct comparisons between our study and that of Wyart
363 et al. (2015), the two sets of findings suggest that space- and feature-based filtering of
364 sensory inputs during evidence accumulation may exhibit different properties. Specifically,
365 sensory evidence accumulation might be restricted to a finite region of space so that under
366 conditions in which signals are sufficiently separated they engage independent
367 accumulators.

368 Interestingly, across both experiments, having participants divide attention between
369 two potential target colours yielded no behavioural cost relative to having them focus on a
370 single target colour. In addition, there was no evidence of a cost for switching between
371 target colours across two epochs, compared with trials in which the two colours repeated.
372 Since in the present study the target colour patches were rendered increasingly visible over

a prolonged time interval and the responses were not speeded, it is possible that our paradigm was insensitive to potential behavioural costs of dividing attention (but see, e.g., Eimer and Grubert, 2014; Grubert et al., 2017). On the other hand, the neural correlates of decision making, as characterised by the onset latency, slope, and peak CPP amplitude, were consistent with the behavioural findings: the CPP time-traces were virtually identical for one- and two-target colour trials in both experiments. As the specifics of our experimental design prevent any strong conclusions, these findings call for further investigation.

In both experiments, we also found a significant serial order bias with higher decision weights for the first target epoch relative to the second. Whereas, in Experiment 1, higher target weights were accompanied by lower distractor weights, in Experiment 2 the weights for both target and distractor signals were higher in the first than the second epoch. This primacy effect was not expected and, in fact, studies using similar paradigms typically reported either no order effects or even the opposite, recency effects (16,40,41). Mirroring the behavioural primacy effects, the colour-locked peak CPP amplitude was higher for the first than the second epoch. By contrast, analyses of the motion-locked CPP in Experiment 2 revealed no order effects. These results suggest that the primacy effects might be related to processing colours rather than motion. Since previous studies did not modulate attention-related signals in the way we did here, the primacy effects we observed are not necessarily inconsistent with the literature. Further studies will be necessary to characterise this effect in more detail.

394 The motion averaging task we have introduced here has potential as a tool for
395 investigating the mechanisms underlying more complex, integrated decision-making.
396 Dynamic weighting of individual decisions to inform a single, integrated decision is
397 ubiquitous in daily life: for example, when deciding whether or not to cross a busy road. In
398 our task, individual motion signals are uncorrelated and, considered in isolation, are not
399 predictive of the final decision. Hence, the averaging task permits independent
400 parameterisation of both *simple* and *integrative* decision-making processes in a
401 straightforward and well characterised motion discrimination task. Using neuroimaging
402 methods with high spatial resolution such as fMRI, future studies could identify the brain
403 areas involved in simple decision-making, on the one hand, and integrative decision-making,
404 on the other. Using this task to characterise decision-making across the lifespan or in clinical
405 groups could shed light on the development of integrative decision-making abilities which
406 are a hallmark of adaptive, intelligent behaviour.

407 *Materials and Methods*

408 **Participants.** Seventy-two healthy volunteers (39 females, average age 21.5 ± 2.5
409 years, 36 per experiment) participated in the study after providing written informed
410 consent. All had normal or corrected-to-normal visual acuity and normal colour vision. In
411 Experiment 1, three participants were identified as outliers based on their behavioural
412 performance and/or EEG signals (see below for details). Data from five participants were
413 removed from Experiment 2, based on the same criteria, leaving 33 and 31 participants per
414 experiment, respectively. The study was approved by the Human Research Ethics

415 Committee of The University of Queensland (approval nr. 2016001247), and was conducted
416 in accordance with the Human Subjects Guidelines of the Declaration of Helsinki.

417 **Stimuli, task and procedure.** In Experiment 1, participants were asked to monitor
418 *three* successively presented epochs of coherent motion within each trial, and to indicate
419 the average direction of *two* target-motion events at the end of the trial using a response
420 dial. A response feedback symbol showing the correct answer was presented after every
421 trial.

422 At the beginning of each trial, a central disk cued participants to the target colour to
423 monitor for during the upcoming trial (Fig. 1a). Different colours were counterbalanced
424 across participants. The cue was followed by a buffer period showing a field of 80 grey,
425 randomly-moving dots. The dots' colour saturation gradually increased before returning to
426 grey (Fig. 1b). The increase in saturation revealed two overlapping, coloured-dot patches
427 moving in different directions. Each trial consisted of three epochs – in two of these epochs
428 one dot patch was rendered in the target colour, and the other appeared in a distractor
429 colour. Target patches were displayed equally often in the first, second and third epochs of
430 a trial. In the remaining (no target/distractor only) epoch, neither of the patches had a
431 target colour.

432 To characterise potential effects of the number of task-relevant colours to be
433 monitored, in separate blocks of trials participants were cued to look for either one target
434 colour (e.g., blue), or two different target colours (e.g., blue and yellow). In two target-
435 colour trials, there was an equal numbers of trials in which the target colour repeated or
436 changed between two target-present epochs within the trial. For each participant, distractor

437 colours were always different from target colours. Combinations of target and distractor
438 colours were counterbalanced across participants.

439 Dot-motion was generated at a suprathreshold level (40% coherence), with a speed
440 of 19°/s, 100 ms dot-life, and with different signal-dots across frames and random-walk
441 noise-dots (23). Although coherent motion was present throughout the epoch (1.5 s, Fig.
442 1b), different motion directions were discernible only at higher colour saturations. The
443 motion directions were uniformly sampled from 0°–359°, with the target-distractor and
444 target-target difference remaining within 30°–150°. Five easily distinguishable colours (Fig.
445 1b) were selected in the HSL colour-space with a minimum hue difference of 72° and
446 medium saturation and brightness (50). Two randomly-selected colours served as targets
447 and two as distractors. Participants completed 30 practice trials followed by six blocks of 44
448 trials (264 trials in total). Each experimental session lasted approximately one hour.

449 In Experiment 2, to measure responses to targets and distractors independently, the
450 dot fields corresponding to target and distractor signals flickered (ON-OFF) concurrently at
451 different frequencies (12 and 18 Hz). The pairing between a given frequency and stimulus
452 type (target vs. distractor) was counterbalanced across trials. The introduction of these
453 flickering displays yielded distinct, time-resolved steady-state evoked potentials (SSVEPs,
454 see Norcia *et al.*, 2015), which enabled us to read out the strength of target and distractor
455 representations on each trial. To optimise the display for recording SSVEPs, the field size,
456 dot size and dot number were doubled in Experiment 2 (Fig. 3a) relative to Experiment 1.
457 The dot-motion was generated at 2.5°/s, with an infinite dot life. Three distinctive colours
458 (maximum saturation 75, minimum colour separation 90°, Fig. 3a) were selected; two

459 colours served as targets, and the remaining one served as a distractor. The distractor and
460 target colours were counterbalanced across participants. The colour saturation increased
461 rapidly (.25 s) from grey to full saturation, and remained at maximum saturation for 1 s. In
462 contrast to Experiment 1, in which three epochs of coloured dots were shown, in
463 Experiment 2 only two epochs of dots were shown, and both epochs within a trial contained
464 a target-motion patch (i.e., there was no longer a no target/distractor only epoch). Coherent
465 motion events were presented for .5 s during the maximum saturation period, and at
466 variable times (.50–.75 s asynchrony relative to the onset of colour modulation).
467 Participants completed 64 practice trials followed by six blocks of 64 trials (384 trials in
468 total). All other details were the same as in Experiment 1.

469 **Apparatus.** The experiments were conducted in a dark, acoustically and
470 electromagnetically shielded room. The stimuli were presented on a 24" monitor with
471 1920×1080 resolution and a refresh rate of 144 Hz. The experimental software was custom-
472 coded in Python using the PsychoPy (25,26) toolbox. EEG signals were recorded using 64 Ag-
473 AgCl electrodes (BioSemi ActiveTwo) arranged in the 10-20 layout, and sampled at 1,024 Hz.

474 **Behavioural analyses.** To identify outlier participants, the distributions of error
475 magnitudes (i.e., the angular difference between the response and the correct answer)
476 were compared to a uniform distribution (i.e., pure guessing) using the Kolmogorov-Smirnov
477 test. Participants for whom the probability of the null hypothesis (i.e., a uniform distribution
478 of error magnitudes) exceeded .001 were removed from further analyses. The remaining
479 distributions per experimental condition and per participant were fitted to a theoretical
480 model (27), and responses were separated into noisy target responses and random guesses.

481 To quantify decision weights, a multiple-regression (OLS) model with a term for each of the
482 presented motion directions, expressed as complex numbers, was fitted to the responses,
483 separately per participant and experimental condition. The absolute value of the resulting
484 regression coefficients reflects the influence of each of the presented coherent motion
485 signals on the response, i.e., its *decision weight*. As the decision weights were always
486 positive, we used permutation test (10,000 permutations) to generate the empirical null
487 distribution against which the empirical decision weights were tested.

488 **EEG analyses.** EEG signals were analysed using the MNE-Python (28) toolbox. The
489 data were offline re-referenced to the average electrode, low-pass filtered at 99 Hz and
490 notch-filtered at 50 Hz to eliminate line noise. The recorded signal was pre-processed using
491 the FASTER (29) algorithm for automated artefact rejection. The pre-processed signal was
492 down-sampled to 256 Hz, segmented into epochs between the cue-onset and the response-
493 display onset, baseline-corrected relative to -.1–0 s pre-trial and linearly de-trended. Outlier
494 epochs and participants were identified using the FASTER algorithm and removed from
495 further analyses.

496 To characterise the temporal dynamics of evidence accumulation, we quantified the
497 onset latency, slope and peak amplitude of an ERP known as the central-parietal positivity
498 (CPP). Previous research has shown that the time-course of the CPP closely resembles the
499 time-course of evidence accumulation: specifically, its amplitude builds up gradually (8), the
500 build-up slope is proportional to stimulus quality (9), and it is observed even in the absence
501 of overt responses (10). The CPP ERP was computed by averaging Cz/CPz electrodes across
502 trials. Each epoch within a trial was extracted from the onset of the increase in colour

503 saturation and baseline-corrected relative to a common baseline during -.1–0 s, averaged
504 across all epochs. The peak CPP amplitudes were identified using the jackknife-method (30).
505 Using the same method, ERP onset latencies were computed at 50% peak amplitude. The
506 ERP slopes were computed as the amplitude difference between -.05 s and .05 s relative to
507 the ERP onset, and divided by .1 s so as to yield μV/s.

508 Time-resolved SSVEP power at tagged frequencies was computed using Morlet
509 wavelets with fixed-width .5 s Gaussian taper, and normalized relative to the neighbouring
510 frequencies. The mean power per epoch was computed during the 1 s of maximal colour
511 saturation. For analyses of the target and distractor SSVEPs, the power per epoch was
512 baseline-corrected relative to a .1 s interval around the onset of maximal colour saturation
513 (.5 and 2.5 s, for the first and the second epochs, respectively).
514

515 *References*


516 1. Forstmann BU, Ratcliff R, Wagenmakers E-J. Sequential Sampling Models in Cognitive Neuroscience:
517 Advantages, Applications, and Extensions. Annu Rev Psychol. 2016;67(1):641–66.

518 2. Ratcliff R, Smith PL, Brown SD, McKoon G. Diffusion Decision Model: Current Issues and History. Trends
519 Cogn Sci. 2016 Apr 1;20(4):260–81.

520 3. O'Connell RG, Shadlen MN, Wong-Lin K, Kelly SP. Bridging Neural and Computational Viewpoints on
521 Perceptual Decision-Making. Trends Neurosci. 2018 Nov 1;41(11):838–52.

522 4. Shadlen MN, Kiani R. Decision Making as a Window on Cognition. Neuron. 2013 Oct 30;80(3):791–806.

523 5. Heekeren HR, Marrett S, Ungerleider LG. The neural systems that mediate human perceptual decision
524 making. Nat Rev Neurosci. 2008 Jun;9(6):467–79.

525 6. Ratcliff R, Philiastides MG, Sajda P. Quality of evidence for perceptual decision making is indexed by trial-
526 to-trial variability of the EEG. Proc Natl Acad Sci. 2009 Apr 21;106(16):6539–44.

527 7. Liu T, Pleskac TJ. Neural correlates of evidence accumulation in a perceptual decision task. J
528 Neurophysiol. 2011 Aug 17;106(5):2383–98.

529 8. O'Connell RG, Dockree PM, Kelly SP. A supramodal accumulation-to-bound signal that determines
530 perceptual decisions in humans. Nat Neurosci. 2012 Dec;15(12):1729–35.

531 9. Kelly SP, O'Connell RG. Internal and External Influences on the Rate of Sensory Evidence Accumulation in
532 the Human Brain. J Neurosci. 2013 Dec 11;33(50):19434–41.

533 10. Twomey DM, Kelly SP, O'Connell RG. Abstract and Effector-Selective Decision Signals Exhibit Qualitatively
534 Distinct Dynamics before Delayed Perceptual Reports. J Neurosci. 2016 Jul 13;36(28):7346–52.

535 11. Hanks TD, Summerfield C. Perceptual Decision Making in Rodents, Monkeys, and Humans. Neuron. 2017
536 Jan 4;93(1):15–31.

537 12. Summerfield C, Tsetsos K. Do humans make good decisions? Trends Cogn Sci. 2015 Jan 1;19(1):27–34.

538 13. Smith PL, Ratcliff R. An integrated theory of attention and decision making in visual signal detection.
539 Psychol Rev. 2009 Apr;116(2):283–317.

540 14. Leite FP, Ratcliff R. Modeling reaction time and accuracy of multiple-alternative decisions. Atten Percept
541 Psychophys. 2010 Jan 1;72(1):246–73.

542 15. White CN, Ratcliff R, Starns JJ. Diffusion models of the flanker task: Discrete versus gradual attentional
543 selection. Cognit Psychol. 2011 Dec 1;63(4):210–38.

544 16. Wyart V, Myers NE, Summerfield C. Neural Mechanisms of Human Perceptual Choice Under Focused and
545 Divided Attention. J Neurosci. 2015 Feb 25;35(8):3485–98.

546 17. Churchland AK, Kiani R, Shadlen MN. Decision-making with multiple alternatives. Nat Neurosci. 2008
547 Jun;11(6):693–702.

548 18. Churchland AK, Ditterich J. New advances in understanding decisions among multiple alternatives. Curr
549 Opin Neurobiol. 2012 Dec 1;22(6):920–6.

550 19. Spitzer B, Blankenburg F, Summerfield C. Rhythmic gain control during supramodal integration of
551 approximate number. NeuroImage. 2016 Apr 1;129:470–9.

552 20. Spitzer B, Waschke L, Summerfield C. Selective overweighting of larger magnitudes during noisy
553 numerical comparison. Nat Hum Behav. 2017 Aug;1(8):0145.

554 21. Itthipuripat S, Cha K, Deering S, Salazar AM, Serences JT. Having More Choices Changes How Human
555 Observers Weight Stable Sensory Evidence. J Neurosci. 2018 Oct 3;38(40):8635–49.

556 22. Kohl C, Spieser L, Forster B, Bestmann S, Yarrow K. The Neurodynamic Decision Variable in Human Multi-
557 alternative Perceptual Choice. J Cogn Neurosci. 2018 Oct 2;31(2):262–77.

558 23. Scase MO, Braddick OJ, Raymond JE. What is Noise for the Motion System? Vision Res. 1996
559 Aug;36(16):2579–86.

560 24. Norcia AM, Appelbaum LG, Ales JM, Cottereau BR, Rossion B. The steady-state visual evoked potential in
561 vision research: A review. J Vis. 2015 May 1;15(6):4–4.

562 25. Peirce JW. PsychoPy—Psychophysics software in Python. J Neurosci Methods. 2007 May 15;162(1–2):8–
563 13.

564 26. Peirce JW. Generating Stimuli for Neuroscience Using PsychoPy. Front Neuroinformatics [Internet]. 2009
565 Jan 15 [cited 2012 Dec 5];2. Available from: http://www.ncbi.nlm.nih.gov/pmc/articles/PMC2636899/

566 27. Schneegans S, Bays PM. No fixed item limit in visuospatial working memory. Cortex. 2016 Oct
567 1;83(Supplement C):181–93.

568 28. Gramfort A, Luessi M, Larson E, Engemann DA, Strohmeier D, Brodbeck C, et al. MEG and EEG data
569 analysis with MNE-Python. Front Neurosci [Internet]. 2013 Dec 26 [cited 2017 Dec 20];7. Available from:
570 https://www.ncbi.nlm.nih.gov/pmc/articles/PMC3872725/

571 29. Nolan H, Whelan R, Reilly RB. FASTER: Fully Automated Statistical Thresholding for EEG artifact Rejection.
572 J Neurosci Methods. 2010 Sep 30;192(1):152–62.

573 30. Ulrich R, Miller J. Using the jackknife-based scoring method for measuring LRP onset effects in factorial
574 designs. Psychophysiology. 2001;38(5):816–827.

575 31. Treue S, Hol K, Rauber H-J. Seeing multiple directions of motion—physiology and psychophysics. Nat
576 Neurosci. 2000 Mar;3(3):270–6.

577 32. Loughnane GM, Newman DP, Bellgrove MA, Lalor EC, Kelly SP, O'Connell RG. Target Selection Signals
578 Influence Perceptual Decisions by Modulating the Onset and Rate of Evidence Accumulation. Curr Biol.
579 2016 Feb 22;26(4):496–502.

580 33. Morey RD. Confidence intervals from normalized data: A correction to Cousineau. In: Tutorials in
581 Quantitative Methods for Psychology , 4. 2008. p. 61–64.

582 34. Andersen SK, Müller MM. Behavioral performance follows the time course of neural facilitation and
583 suppression during cued shifts of feature-selective attention. Proc Natl Acad Sci. 2010 Aug
584 3;107(31):13878–82.

585 35. Andersen SK, Müller MM, Hillyard SA. Attentional Selection of Feature Conjunctions Is Accomplished by
586 Parallel and Independent Selection of Single Features. J Neurosci. 2015 Jul 8;35(27):9912–9.

587 36. Gold JI, Shadlen MN. The Neural Basis of Decision Making. Annu Rev Neurosci. 2007;30(1):535–74.

588 37. Eriksen CW. The flankers task and response competition: A useful tool for investigating a variety of
589 cognitive problems. Vis Cogn. 1995;2(2).

590 38. Grubert A, Fahrenfort J, Olivers CNL, Eimer M. Rapid top-down control over template-guided attention
591 shifts to multiple objects. NeuroImage. 2017 Feb 1;146(Supplement C):843–58.

592 39. Eimer M, Grubert A. Spatial Attention Can Be Allocated Rapidly and in Parallel to New Visual Objects. Curr
593 Biol. 2014 Jan 20;24(2):193–8.

594 40. Wyart V, de Gardelle V, Scholl J, Summerfield C. Rhythmic Fluctuations in Evidence Accumulation during
595 Decision Making in the Human Brain. Neuron. 2012 Nov 21;76(4):847–58.

596 41. Cheadle S, Wyart V, Tsetsos K, Myers N, de Gardelle V, Herce Castañón S, et al. Adaptive Gain Control
597 during Human Perceptual Choice. Neuron. 2014 Mar 19;81(6):1429–41.

598